

# Synthesis of nonuniform long-period optical gratings with a continuous refractive index profile

O.V. Kolokoltsev<sup>a,\*</sup>, V.A. Svyryd<sup>b</sup>, I.F. Llamas<sup>b</sup>, and C.L. Ordóñez Romero<sup>a</sup>

<sup>a</sup> *Universidad Nacional Autónoma de México (UNAM), CCADET,*

*Apartado Postal 70-186, 04510, CD Universitaria, México, D.F.,*

<sup>b</sup> *UNAM, Facultad de Ingeniería, CD Universitaria, México, D.F.*

Recibido el 11 de abril de 2005; aceptado el 5 de septiembre de 2005

In this work we present a new method for such a non-trivial problem as the synthesis of optical filters based on non-uniform Long-Period Fiber Gratings (LPGs). The method is based on a real-coded genetic algorithm (GA) with a new quasi-analytical procedure for solving the Zakharov-Shabat Inverse Problem. The method possesses an improved computational stability compared to classic numerical algorithms. The main peculiarity of the non-uniform LPG transmission gratings, compared to the Bragg gratings, is that their optical fields oscillate rapidly. However, the quasi-analytical approach proposed allows one to reduce to a minimum the number of sampling points, without, at the same time, losing accuracy in the solution, *i.e.* the method possesses an improved efficiency. The algorithm convergence was also improved by using the relations of the law of conservation of energy between the interacting waves. It has been shown that the algorithm works adequately even for the case of strongly over-coupled co-propagating lightwave modes, as we demonstrate in several examples of the synthesis of ultra-wide pass-band optical filters (FWHM of 100-200 nm).

*Keywords:* Long-period fiber gratings; synthesis; optical filters; genetic algorithm.

En este trabajo presentamos un nuevo método para un problema no-trivial como la síntesis de filtros ópticos basados en rejillas de periodo largo (Long-Period Fiber Gratings o LPGs) no uniforme. El método esta basado en un código de algoritmo genético real (GA) con un nuevo procedimiento cuasi-analítico para la solución del problema inverso de Zakharov-Shabat. El método posee un estabilidad de computo mejorada compara con los algoritmos numéricos clásicos. La principal peculiaridad de la no uniformidad de las rejillas de transmisión LPG, comparado con las rejillas de Bragg, es que sus campos ópticos oscilan rápidamente. Sin embargo, la aproximación cuasi-analítica propuesta permite reducir al mínimo el número de puntos muestreados, pero, al mismo tiempo, no pierde la precisión en la solución, es decir, el método posee una eficiencia mejorada. La convergencia del algoritmo también fue mejorada usando las relaciones de la ley de conservación de la energía entre las ondas que interactúan. Esto ha mostrado que el algoritmo trabaja adecuadamente aun para los casos de modos de ondas luminosas de más fuerte co-propagación sobre acoplada, como se demuestra en varios ejemplos en la síntesis de filtros de banda de paso óptica ultra-ancha (FWHM de 100-200nm).

*Descriptores:* Rejillas en fibras de periodo largo; síntesis; filtros ópticos; algoritmo genético.

PACS: 42.81.Qb

## 1. Introduction

The problem of optical waveguide grating synthesis initially concentrated on the well-known optical Bragg Grating Reflectors (BGR) based on short-period perturbations of the refractive index in optical waveguides. Their main applications are the narrow GHz-bandwidth optical filters with a desired spectral response for high density WDM fiber optic communications, as well as distributed optical fiber sensors of strain, temperature, etc. [1,2]. In the latter case, the aim of the synthesis problem is to reconstruct the spatially distributed physical forces from an experimental grating spectrum. At the same time, recent studies have shown that so-called Long Period Gratings (LPGs) in some cases possess certain advantages over BGR [3-8]. First of all, they do not require high resolution writing technologies because of their long period ( $\Lambda$ ) that lies between 200 – 800  $\mu\text{m}$ . LPGs are also attractive because of their extended functionality. They are based on the grating induced coupling between co-propagating optical waves; hence, they act as a transmission device. In single mode optical fibers, for example, the grating written in the core by deep UV causes an energy exchange between a fundamental core mode and cladding modes [3]. It

is obvious that the cladding mode fields are very sensitive to changes in the refractive index of the external medium surrounding the fiber. This property, hence, can be used for the distributed sensing of some liquids, as well as gases, using chemically active cover layers in the latter case. The sensitivity of any LPG sensor can be very high because of the long interaction length, 0.1–2 m, and differential response of the interacting modes to the external perturbations. The reciprocal character of the coupled co-propagating lightwave pair allows one, for example, to achieve a simple Mach-Zehnder interferometric sensor structure, in just a single optical fiber [6]. Also, LPGs play a very important role in the photonic technologies operating as a gain equalizing filter in erbium-doped fiber amplifiers (EDFA) [7,8].

The history of the synthesis of guided wave optical filters is associated with the well-known Digital Filters Concepts, which involve the Z-Transforms for the design of Moving Average (MA), Autoregressive (AR), and mixed ARMA filters. Such devices present optical lattice circuits consisting of waveguide elements such as classic Mach-Zehnder interferometers and ring resonators [9]. Later, it was shown that non-uniform Bragg gratings are capable of providing any com-

plex spectral response, and great attention has been paid to the development of new synthesis concepts for them. A variety of inverse scattering (IS) methods have been developed to find a topology of non-uniform BGR that can satisfy a certain desired spectral response. A complex longitudinal profile of weak gratings with the reflection coefficient  $r(\delta) < 1$ , where  $\delta$  is the wavenumber mismatch parameter, can successfully be obtained within the Born (first-order) approach by means of the corresponding inverse Fourier transform of  $r(\delta)$  [10]. The second group of methods is based on the famous Gelfand-Levitan-Marchenko (GLM) integral equations, which provide exact solutions to the Zakharov-Shabat (Z-S) IS problem, expressed through the coupled mode equations and their derivatives [11,12]. Basically, the algorithms developed for GLM use the relation between the coupling function ( $Q$ ), that reflects longitudinal variation of the grating parameters to be found, and the grating impulse response. The main inconvenience of these methods is their low computational efficiency caused by the complexity of the integral equation system. In the general case, it is solved numerically [13,14]. First Kay [15], and then Frangos and Jaggard [16] showed an original way to transform the coupled GLM system to ordinary linear differential equations, leading to an exact analytical solution for  $Q$ . Unfortunately, those algorithms require the target spectral response to be expressed through rational functions, which is far from most practical situations. Also, since GLM is an exact method, it will generate a grating with infinite length. These difficulties have been overcome by E. Perel [17], who developed an iterative algorithm for GLM equations (IA) that, in principle, has no limitations in producing any spectral response. The method is built on a series of multiple integrals, which describe multiple reflections inside the grating. It should be noted that the integral order and, hence, the algorithm complexity grow as the reflectivity BGR approaches unity. Recently, the differential IS algorithms known as discrete layer-peeling (DLP) [18,19] and a continuous layer-peeling (CLP) [20,21] were proposed. These methods have been shown to be very powerful and fast synthesis tools for BGR. The third, most practical group of direct methods involves evolutionary algorithms such as a genetic algorithm (GA) [2,22,23]. GA-based techniques are physically and mathematically transparent, since they use standard direct integration of wave equations. Their main advantage is a result of the possibility of giving a desired weight to most important parts or parameters of the spectral response, in each specific practical case. The drawback of GA is its slow convergence, compared to the layer-peeling algorithms, whenever one needs to obtain a solution close to an ideal one. However, its main strength is a complete freedom in the choice of mathematical methods to optimize the integration algorithms, and the possibility of obtaining the optimal solution within the given technological limitations for the structure, for example, if the filter length should be truncated.

In this work we present a new version of GA optimized for the synthesis of optical band-pass filters based on non-

uniform LPG with a continuous variation in the refractive index profile. In contrast to the case of BGR, the synthesis of Long Period Gratings is respectively a new problem. Although, in principle, all the methods mentioned above are applicable to the synthesis of LPG, this has only been done by DLP on the basis of a segmented LPG in [19], and for a binary-chirped grating in the framework of GLM concept, involving a GA optimization [6]. However, LPGs with a continuously non-uniform refractive index profile that can provide ultra-wide filter frequency response have not been considered. Here, we describe a very simple and efficient algorithm for this case.

## 2. Problem definition

Some comments should be made, first, to describe the algorithm to be considered here. Although the equations for counter-propagated (BGR) and co-propagated (LPG) waves are similar, there is a significant difference in their integration algorithm. First, for the characterization of the reflection gratings, it is sufficient to operate with the reflection coefficient ( $r$ ) given by a relation between the incident and reflected wave amplitudes, *i.e.* the solution does not require a separate description of these waves. Second, even close to the Bragg resonance condition, local spectra of  $r$  are smooth saturating functions ( $|r| < 1$ ) of the propagation coordinate ( $z$ ) and the mismatch  $\delta$ . In contrast, when the waves in LPG are almost phase-matched, the local scattering coefficient  $\rho(\delta, z)$ , determined as the relation of co-propagating waves, oscillates along  $z$ , and can possess peaked-like discontinuities, for loss-less grating with strong wave coupling. In turn, this can lead to computational errors when using IA, DLP, CLP, since their algorithms extensively use the inverse Fourier transform of  $r(z, \delta)$ , or  $\rho(\delta, z)$ . It should also be noted that DLP cannot, in principle, be applied to the synthesis of the wide-band filters, with FWHM of 10-100 nm, since its physical model requires the presentation of the structure as a chain of uniform elementary gratings. The problem is that, for the wide-band filter, each element (or segment) should contain only a few grating periods, and, therefore, the conventional analytical description of the single segment response, used in the transfer matrix technique applied in DLP, is no longer valid here.

A GA presented here allows us to overcome this problem. It is optimized to be very stable even for short-length LPG with 100%-transmittivity that requires high and rapidly varying values of the scattering coefficient with respect to the grating period. Here we consider LPG written in the fiber core as a quasi-sinusoidal perturbation of the refractive index with the amplitude  $\Delta n(z)$  that is varied along the propagation coordinate  $z$ :

$$n(z) = n_b + \Delta n(z) \cos(2\pi z/\Lambda + \theta(z)). \quad (1)$$

Here,  $\Lambda$  denotes the grating fundamental period that can be locally shifted in the space by the function  $\theta$  (local chirping

parameter), and  $n_b$  is the background refraction index change that can be induced in the core. Here, however,  $\theta$  and  $n_b$  are considered to be zero. The substitution of Eq.(1) into the Maxwell equations under the slowly varying amplitude approach gives the following Z-S system:

$$\begin{aligned}\frac{\partial \tilde{u}(z, \delta)}{\partial z} &= j\frac{\delta}{2}\tilde{u}(z, \delta) + jQ(z)\tilde{v}(z, \delta) \\ \frac{\partial \tilde{v}(z, \delta)}{\partial z} &= -j\frac{\delta}{2}\tilde{v}(z, \delta) + jQ^*(z)\tilde{u}(z, \delta),\end{aligned}\quad (2)$$

describing the coupling between the complex amplitudes of the core  $u = \tilde{u} \exp(-j\delta z/2)$  and cladding  $v = \tilde{v} \exp(j\delta z/2)$  modes, co-propagating in the  $z$  direction with the propagation constants  $\beta_u$ , and  $\beta_v$  correspondingly. In Eq. (2)  $\delta$  denotes the wavenumber miss-match  $\delta = \Delta\beta - 2\pi/\Lambda$ ,  $\Delta\beta = \beta_u - \beta_v = 2\pi(n_{core}(\lambda) - n_{clad}(\lambda))/\lambda \approx 2\pi\Delta n_{cc}/\lambda$ , where the typical effective refractive-index difference between the  $u$  and  $v$  modes  $\Delta n_{cc} = 0.002$ ,  $\lambda$  is the optical wavelength;  $Q(z)$  is the envelope of the local coupling coefficient  $q(z) = Q(z) \cos(2\pi z/\Lambda + \theta(z))$ . For single mode optical fibers the coupling function  $Q(z) = Q^*(z) = (\pi/\lambda)I\Delta n(z)$ , where  $I$  is the mode overlap integral, and  $I\Delta n$  is the induced effective index perturbation that can reach  $3.0 \times 10^{-3}$  [3]. It is assumed that the incident lightwave can excite in LPG the fundamental core mode with spectral characteristic  $u(0, \delta) = u_0$ , and the desired output spectral response for the cladding mode is given by  $v(L, \delta) = s(\delta)$ , where  $L$  is the grating length. It is convenient to reformulate Eq.(2) to the Riccati equation by introducing the local scattering coefficient  $\rho(z, \delta) = \tilde{v}(z, \delta)/\tilde{u}(z, \delta)$ :

$$\frac{\partial}{\partial z}\rho(z, \delta) = -j\delta\rho(z, \delta) - jQ(z)\rho^2(z, \delta) + jQ(z). \quad (3)$$

Equations (2) and (3) are further used here to find the apodization function  $Q(z)$  that satisfies  $s(\delta)$ , according to the general concept of evolutionary algorithms. The basic principle to do this is the following:

- 1) we need to generate random numbers to form  $Q(z)$ ,
- 2) to calculate  $\tilde{s}(\delta)$  by integration of Eq. (3), and
- 3) to minimize the difference between the calculated ( $\tilde{s}$ ) and desired ( $s$ ) spectra.

### 3. Direct problem

It is possible to show that numerical integration of Eq. (2) or (3) by conventional methods, for example, like a fourth-order Runge-Kutta technique proposed for CLP [20,21], does not guarantee the stability of the procedure at a reasonable discretization step  $\Delta z$ . This is true for two reasons. First, when solving the equations numerically, the instability in any numerical algorithm exhibits an amplification effect for  $u$  and  $v$  that takes place when  $\Delta z$  is not sufficiently small compared to the local period of a quasi-periodic energy exchange between the modes, given by  $\ell \approx \pi L^{-1}/\sqrt{0.25\delta^2 + Q^2}$ . For example, if the total grating length  $L = 10$  cm, and  $Q = \delta = 10$  cm<sup>-1</sup>, the number of the discretization points in the grating should be  $N > 10000$  to provide  $\Delta z \ll \ell$  necessary for good convergence of a numerical method. However, this makes the algorithm too slow to be used in the evolutionary methods (note,  $L$ ,  $Q$  and  $\delta$  can be larger). Second, at the condition  $Q\delta \gg 1$ , the local reflection coefficient  $\rho(z, \delta)$  has sharp discontinuities (in the case of uniform grating  $\rho(z, 0) \propto \tan(zQ^{\text{const}})$ ), which give rise to serious computational errors.

To provide a high stability and efficient integration of Eq. (3) we propose to divide the local scattering effect by two steps. Let us suppose that only the pure scattering takes place within a small space interval  $\{z_i, z_{i+1} = z_i + \Delta z\}$ , and that the phase delay effect acts only within the next interval  $\{z_{i+1}, z_{i+2}\}$ . Therefore, the analytical presentation of this two-step mathematical model looks as follows:

$$\begin{cases} \frac{\partial}{\partial z}\rho(z, \delta) = jQ(z) - jQ(z)\rho^2(z, \delta), & (n-1)\Delta z < z < n\Delta z, \\ \frac{\partial}{\partial z}\rho(z, \delta) = -j\delta\rho(z, \delta), & n\Delta z < z < (n+1)\Delta z, \quad n = 1 \dots N. \end{cases} \quad (4)$$

In this case we can operate with the analytical solutions to (4) within the corresponding intervals  $z_i$ :

$$\begin{cases} \rho(z, \delta) = j \tan(2 \int Q(z) dz + C_1), & (n-1)\Delta z < z < n\Delta z, \\ \rho(z, \delta) = C_2 \exp(-j\delta z), & n\Delta z < z < (n+1)\Delta z, \quad n = 1 \dots N. \end{cases} \quad (5)$$

The step-like-variable integration constants  $C_1$  and  $C_2$  in the system (5) have to be redefined at each coordinate  $z_n$  from local initial conditions as:

$$C_2(n\Delta z, \delta) = \rho((n-1)\Delta z, \delta),$$

and

$$C_1(z_n) = -2j \int Q(z_{n-1}) dz + \ln\left(\frac{1 + \rho(z_{n-1}, \delta)}{1 - \rho(z_{n-1}, \delta)}\right). \quad (6)$$

Therefore, at each point  $z_n = 2n\Delta z$ , the solution to Eq. (3) can finally be expressed by:

$$\rho_n(\delta) = \rho_{n-1}(\delta) * P(\delta) = S(Q_n, \rho_{n-1}(\delta)) * P(\delta), \quad (7)$$

where the subscript signifies the current coordinate  $z_n$ ;

$$S(Q_n, \rho_{n-1}(\delta)) = \frac{\exp(\gamma(\delta)) - 1}{\exp(\gamma(\delta)) + 1}$$

with

$$\gamma(\delta) \equiv 2jQ_n\Delta z + \ln\left(\frac{1 + \rho_{n-1}(\delta)}{1 - \rho_{n-1}(\delta)}\right),$$

and  $P(\delta) \equiv \exp(-j\delta\Delta z)$ . Note,

$$\int Q_n dz - \int Q_{n-1} dz \approx Q_n \Delta z,$$

and, also, Eq. (6) are presented in the form suitable for C++ programming.

#### 4. Calculation of spectra

The calculation of the spectrum of the cladding mode  $v(L, \delta) = s(\delta)$  is the important feature in the problem considered. Formally, it can be expressed through the local scattering coefficient  $\rho$  and, also, by involving Eq. (2):

$$v(z, \delta) = \rho(z, \delta)u(z, \delta); \quad (8)$$

where

$$u(z, \delta) = \exp\left(j \int_0^z Q\rho(\tilde{z}, \delta) d\tilde{z}\right), \quad (9)$$

However, the numerical realization of Eq. (8) is accompanied by significant calculation difficulties associated with the discontinuities in  $\rho(z, \delta)$  discussed above. The problem can be overcome by involving the energy conservation law  $|u(\delta)|^2 + |v(\delta)|^2 = \text{Const} = |u_0|^2$  that reduces the problem to the equations

$$|v_n(\delta)|^2 = \frac{|\rho_n(\delta)|^2}{|u_0|^2 + |\rho_n(\delta)|^2},$$

and

$$|u(z, \delta)|^2 = |u_0|^2 - |v(z, \delta)|^2, \quad (10)$$

which have a very smooth function on their right-hand side, and allow us to simulate strongly-overcoupled gratings. In turn, the argument of the waves can be calculated without any problem by Eq. (8). Thus, the complex wave amplitudes can be expressed as follows:

$$v(z, \delta) = |v(z, \delta)| \exp(j \arg(\rho(z, \delta) u(z, \delta))), \quad (11)$$

$$u(z, \delta) = |u(z, \delta)| \exp(j \arg(u(z, \delta))), \quad (12)$$

where the amplitude modulus and arguments are given by Eq. (10) and Eq. (8), respectively. Finally, Eq.(12) can be presented in a discrete form by the above step-like expression for  $\rho(z, \delta)$  and any conventional integration algorithm for Eq. (9).

Figures 1 to 4 show the calibration curves obtained for the uniform grating from Eq. (7-10). As seen from the figures, they are in very good agreement with the data obtained

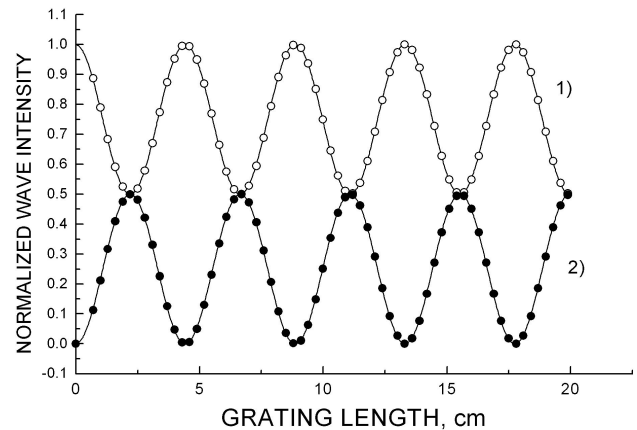


FIGURE 1. The periodical energy exchange between the core 1) and the cladding 2) optic modes in uniform LPG at  $\delta=1.0 \text{ cm}^{-1}$ , and  $Q = 0.5 \text{ cm}^{-1}$ , obtained by our algorithm (continuous curves) and by the exact solution (circles) from Eq. (13). The results present the following relations: 1)  $|u|^2 / |u_0|^2$ , and 2)  $|v|^2 / |u_0|^2$ .

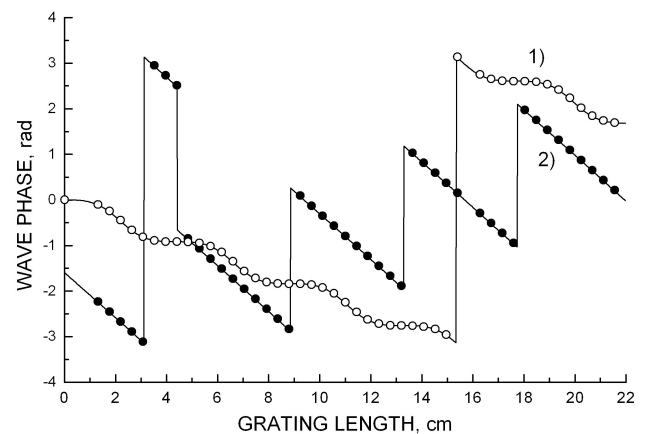


FIGURE 2. The phase evolution of the core 1) and the cladding 2) optic modes in uniform LPG at  $\delta=1.0 \text{ cm}^{-1}$ , and  $Q = 0.5 \text{ cm}^{-1}$ , obtained by our algorithm (continuous curves) and by the exact solution (circles).

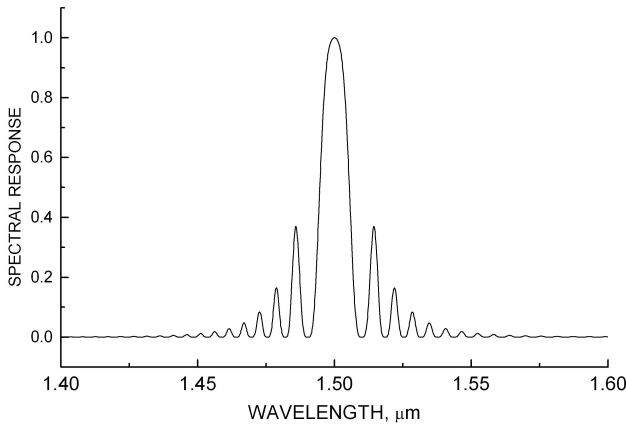


FIGURE 3. The curve shows the normalized intensity of the cladding mode  $|v|^2/|u_0|^2$  calculated by the algorithm at the distance of  $L = 20$  cm in overcoupled uniform LPG with  $Q = 0.5 \text{ cm}^{-1}$ .

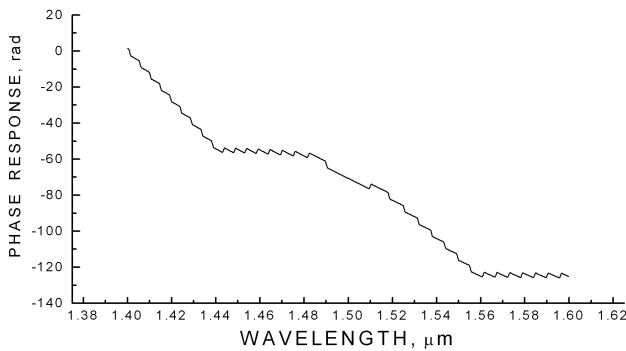


FIGURE 4. The phase response of the cladding mode at the same conditions as in Fig. 3.

by the well-known exact solution for the simple uniform case [26,27]:

$$\begin{aligned} u/u_0 &= [\cos sz - j(\delta/2s) \sin sz] \exp(j0.5\delta z) \\ v/u_0 &= -j(Q/s) \sin sz \exp(-j0.5\delta z), \\ s &= \sqrt{\delta^2/4 + Q^2}. \end{aligned} \tag{13}$$

### 5. Solution of the inverse problem by a genetic algorithm

In the framework of a GA, the synthesis problem can be formulated as finding an optimal  $Q(z)$  that would minimize what is known as the objective function  $\Phi$  within the interval  $\delta_{max} - \delta_{min}$ :

$$\begin{aligned} \Phi &= \int_{\delta_{min}}^{\delta_{max}} (|s(\delta)| - |v(L, \delta)|)^2 d\delta \\ &+ \mu \int_{\delta_{min}}^{\delta_{max}} (\arg(s(\delta)) - \arg(v(L, \delta)))^2 d\delta \rightarrow \min \equiv f, \end{aligned} \tag{14}$$

where the first integral gives the solution for the amplitude spectral response, and  $\mu$  is the weighted coefficient for the

second term that allows one to obtain a desired phase response programmed by  $\arg(s(\delta))$  (in this work  $\mu = 0$ ). In principle,  $Q(z)$  can be modeled by a wide class of functions. We suppose, however, that a more natural way for the case of the band-pass filter is to express  $Q(z)$  with the help of the following series:

$$Q(z) = \sum_{\ell=1}^{M(2,3..m)} \alpha_{\ell} \frac{\sin(\eta_{\ell}z + \psi_{\ell})}{(\eta_{\ell}z + \psi_{\ell})}, \tag{15}$$

since the sinc-like solution is valid for the weak gratings, when

$$\int Q(z) dz < \pi/2.$$

Therefore, the problem is to find the vectors  $\vec{\alpha} = \alpha_0 \dots \alpha_M^T$ ,  $\vec{\eta} = \eta_0 \dots \eta_M^T$ ,  $\vec{\psi} = \psi_0 \dots \psi_M^T$ , which will satisfy  $\Phi \rightarrow f$ .

The above optimization problem was solved by real-coded GA with the standard cyclic computational operations: initialization, mutation, fitness evaluation, and selection of the best individuals (see review [24], or our work [25]). Here, we describe some key operations applied in our version of the GA. Its first step consists in the initialization of normally distributed random numbers forming the first parent generation of the populations  $\vec{\alpha}_{\sigma}$ ,  $\vec{\eta}_{\sigma}$ ,  $\vec{\psi}_{\sigma}$ , where  $\sigma = 1, \dots, \sigma_t$  and the total number of populations  $\sigma_t = 500$ . The evolutionary cycle ( $P$ ) looks as follows. A certain part of the parents ( $\tilde{\sigma}$ ) is selected under the criterion that they provide the smallest values of the objective function  $\Phi$ , to generate what are known as child populations, whose total number ( $\tau$ ) is also equal to  $\sigma_t$ . It is realized by:

- 1) the individual mutation operation

$$\begin{aligned} \tilde{\alpha}_{\tau} &\equiv \alpha_{\tilde{\sigma}} \pm \sum_k \partial \alpha_k, \\ \tilde{\eta}_{\tau} &\equiv \eta_{\tilde{\sigma}} \pm \sum_k \partial \eta_k, \\ \tilde{\psi}_{\tau} &\equiv \psi_{\tilde{\sigma}} \pm \sum_k \partial \psi_k, \end{aligned}$$

where  $\partial \alpha_i, \partial \eta_i, \partial \psi_i \ll \alpha_i, \eta_i, \psi_i$  are normally distributed random numbers;  $\tau = 1, \dots, \sigma_t, \tilde{\sigma} = 1.. \sigma_t/k$  ( $\sigma_t/k$  is a natural number),  $k = 5$  is the number of new individuals obtained by the mutation of each parent; and

- 2) the recombination operation established as

$$\begin{aligned} \tilde{\alpha}_i(new) &= 0.75 \tilde{\alpha}_i + 0.25 \tilde{\alpha}_j, \\ \tilde{\alpha}_j(new) &= 0.75 \tilde{\alpha}_j + 0.25 \tilde{\alpha}_i \end{aligned}$$

(for  $\vec{\eta}_{\sigma}, \vec{\psi}_{\sigma}$  it was done in a similar manner), with the probability decreasing from 0.1 to 0.01 depending on the quality of the individuals participating in

the crossover operation. The next operation is again the selection of the best  $\tilde{\alpha}_\tau, \tilde{\eta}_\tau, \tilde{\psi}_\tau$  by means of the evaluation of the objective function  $\Phi$ . The data obtained in a cycle  $P$  are considered, then, as the parent data in the next cycle  $P+1$ . Note that the mutation step must be decreased each time when the smallest  $\Phi(P) > \Phi(P+1)$ . This loop of the algorithm continues until a smallest  $\Phi \leq f$  or the computing time is exhausted. An acceptable solution can usually be obtained for  $P=30-50$ , which takes 12-15 min with a PIV-class PC.

## 6. Results and discussions

Let us consider the principle steps in the synthesis of LPG band-pass filter with square amplitude spectral response:  $v(L, \delta) = s(\delta) = 1$  within  $\delta_1 < \delta < \delta_2$  (or:  $\lambda_{min} < \lambda < \lambda_{max}$ ) and  $s(\delta) = 0$  elsewhere, at the input condition  $u(0, \delta) = 1$ . It is very important, first, to define proper ranges for randomly generated numbers  $\tilde{\alpha}_\sigma, \tilde{\eta}_\sigma, \tilde{\psi}_\sigma$ . This determines how fast the  $\Phi$  will converge to the global minimum. Here, we are interested in finding the solution for the central filter wavelength  $\lambda_c = 1.5 \mu\text{m}$ . Hence  $\Delta\beta = 2\pi\Delta n_{cc}/\lambda_c = 85 \text{ cm}^{-1}$ , and the condition  $\delta = \Delta\beta + 2\pi/\Lambda = 0$  gives us the fundamental  $\Lambda = 750 \mu\text{m}$ . It is easy to see that the spatial frequency  $\eta$  in (15) determines the deviation in the fundamental period  $\eta \approx (2\pi/\tilde{\Lambda} - 2\pi/\Lambda) \approx d(2\pi/\Lambda)$ . Taking into account the fact that we want to obtain the flat-top transmittance curve of the filter within the given range (in general, it is sufficient to consider any transmittance function), it is reasonable to assume that the grating should simultaneously phase-match the waves within  $\delta_1 < \delta < \delta_2$ , or, at least, at  $\delta = \delta_{1,2}$ . This is equivalent to the condition

$$\begin{aligned} d\delta/d\lambda = 0 &\Rightarrow -2\pi\Delta n_{cc}/\lambda^2 - d(2\pi/\Lambda)/d\lambda = 0, \\ &\Rightarrow \eta \approx 2\pi\Delta n_{cc}(\lambda_{max} - \lambda_{min})/\lambda_c^2. \end{aligned}$$

For example, if  $\Delta\lambda = \lambda_{max} - \lambda_{min} = 200 \text{ nm}$  (ultra-wide band-pass filter)  $\eta \approx 27.8\Delta\lambda = 5.56 \text{ cm}^{-1}$ . Also, it is clear that the grating length  $L$  must be related to the period  $2\pi/\eta$ . In particular, the amplitude response with sharp edges requires  $L \approx 2\pi p/\eta$ , where  $p > 10$ .

The numerical error in the method is mainly associated with the maximal detuning  $\delta$  used in each specific case considered. On the one hand, we are interested in increasing the discretization step  $\Delta z$  to make our GA faster. However, on the other hand, a maximal value of  $\Delta z$  has to be limited by minimal phase delay  $\delta\Delta z$  for each interval  $z_i, z_{i+1}$  to guarantee acceptable accuracy of the algorithm. Since we use the analytical solution within these intervals, this allows us to increase the critical phase delay value up to  $\delta\Delta z \approx \pi/8$ , and, therefore  $\Delta z^{max} \approx \pi/(8\delta)$ . This estimation shows that we can operate only with  $N = L/\Delta z^{max} = 500$  intervals when  $L = 10 \text{ cm}$  and the calculation window is as wide as 500 nm, as required for a wide-band filter. The advantage of such a

discretization is that both wide-band (small  $L$ ), and narrow-band gratings, which possess FWHM  $< 10 \text{ nm}$ , large  $L$ , but narrow calculation window of  $\approx 50 \text{ nm}$ , will be synthesized for equal computing time, and with acceptable accuracy. It is very important to stress that our quasi-analytical two-step scheme presented here is 20-50 times faster than the conventional fourth-order Runge-Kutta algorithm.

The results of the synthesis of the structure with square amplitude spectral responses obtained for  $\Delta\lambda = 200 \text{ nm}$ ,  $100 \text{ nm}$ , and  $10 \text{ nm}$  are presented in Figs. 5 to 17. For all the cases, we used  $N = 600$  spatial intervals  $\Delta z$  when solving the Riccati Eq. (3). As one can see from Figs. 5, 9, and 12, the transmission spectra possess quite sharp transitions at the edges of the band-pass and close to -45 dB suppression of the signal lying out of the operation transmission band (as an example see Fig. 6). Such a solution can be referred to "ideal", taking into account that the curves lie very close to the target square response. The coupling functions  $Q(z)$  shown in Figs. 7, 10, and 13 providing these as "ideal" results were synthesized at  $M = 40$ , the *sinc* terms in Eq. (15). Although the results seem to be more than satisfactory from the mathematical point of view, there is a very important point to be discussed here. Figures 8 and 11, which present the spatial evolution of the scattered mode within the the pass-band in the case of ultra wide-band "ideal" filters, demonstrate that within initial short part of the grating there is a 100%-energy exchange between the modes and, moreover, the scattered mode oscillates too quickly. If we estimate the period of the mode oscillation, we can see that it is comparable with only a few grating periods. Hence, it is obvious, the physical realization of the corresponding coupling functions is very problematic, because the existing UV writing technologies for the optical fiber gratings cannot provide such a rapid growth in the induced refractive index, within two-three grating periods, as required for the synthesized  $Q(s)$  describing the "ideal" ultra-wide band-pass filters. Note that in the case of the narrow-band filter ( $\Delta\lambda = 10 \text{ nm}$ ) both the mode spatial evolution shown in Fig. 14 and the coupling function in Fig. 13 vary sufficiently slowly and can be realized technologically.

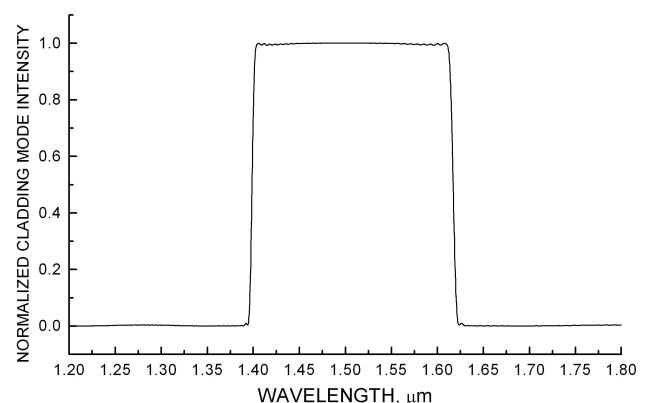


FIGURE 5. The synthesized spectrum presents the normalized intensity of the cladding mode  $|v(L, \lambda)|^2 / |u_0|^2$ . The LPG length  $L = 20 \text{ cm}$ .

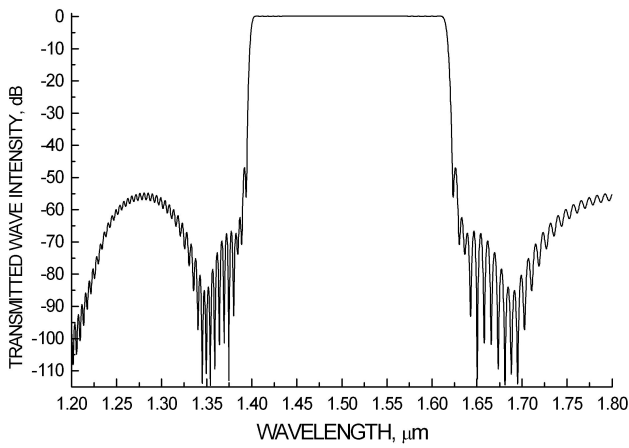


FIGURE 6. The logarithmic scale of the spectrum presented in Fig. 5.

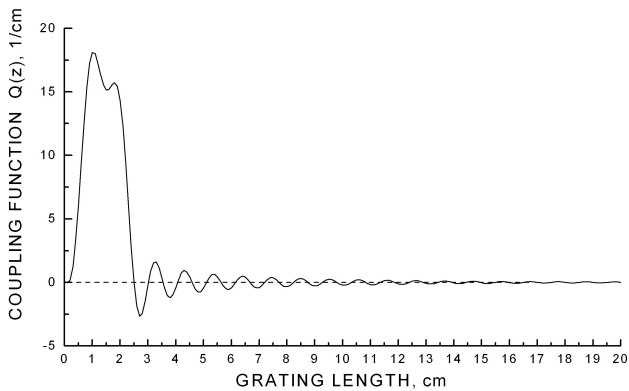


FIGURE 7. The synthesized coupling function  $Q(z)$  providing the spectrum shown in Figs. 5 and 6.

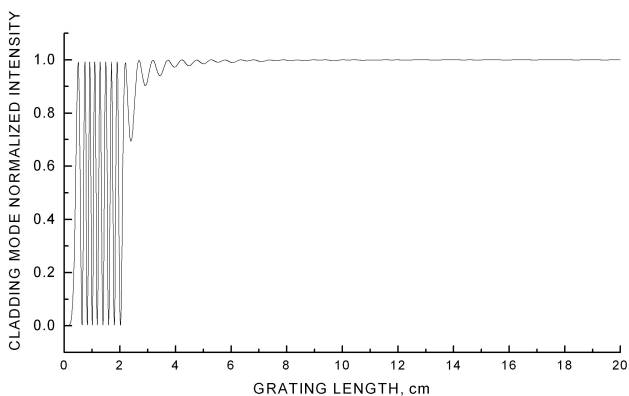


FIGURE 8. The spatial evolution of the cladding mode in non-uniform LPG at  $\delta = 0.01 \text{ cm}^{-1}$ , and the coupling function  $Q(z)$  shown in Fig. 7. The curve presents  $|v(z)|^2 / |u_0|^2$ .

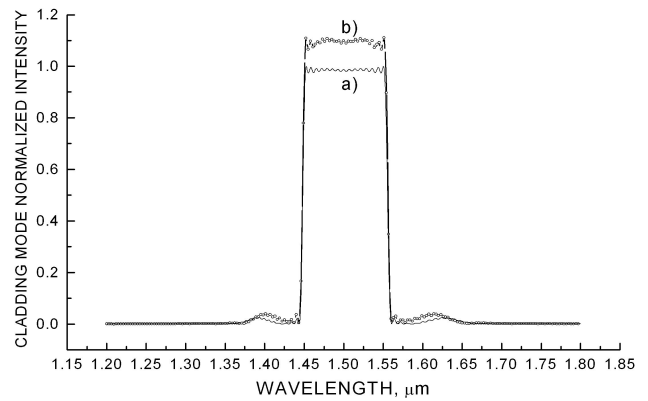


FIGURE 9. The spectra of the cladding mode a) calculated by our method, and b) calculated by fourth-order Runge-Kutta numerical method with the coupling function synthesized with the help of the GA that is shown in Fig.(10, curve (a)). The grating length  $L = 20 \text{ cm}$ .

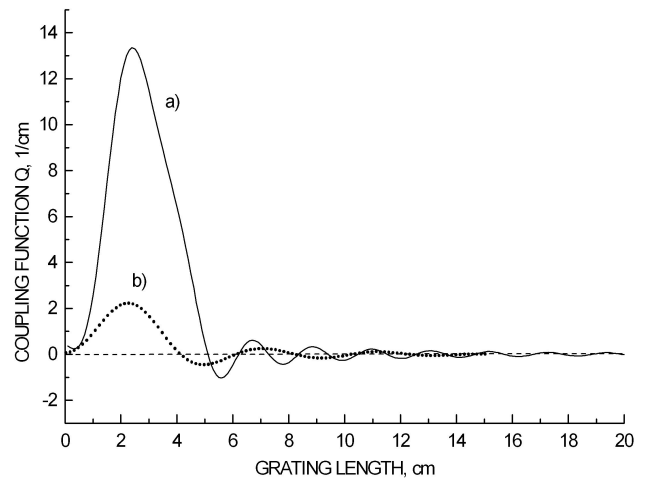


FIGURE 10. The synthesized coupling function  $Q(z)$  providing the spectra shown in Fig. 9. For the comparison the curve b) shows  $Q(z)$  for the “realizable” filter presented in Fig. 15.

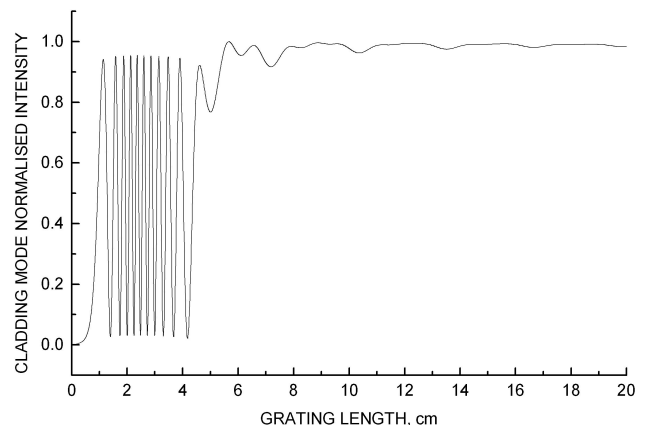


FIGURE 11. The spatial evolution of the cladding mode  $(|v(z)|^2 / |u_0|^2)$  in non-uniform LPG at  $\delta = 0.01 \text{ cm}^{-1}$ , for the coupling function  $Q(z)$  shown in Fig. 10.

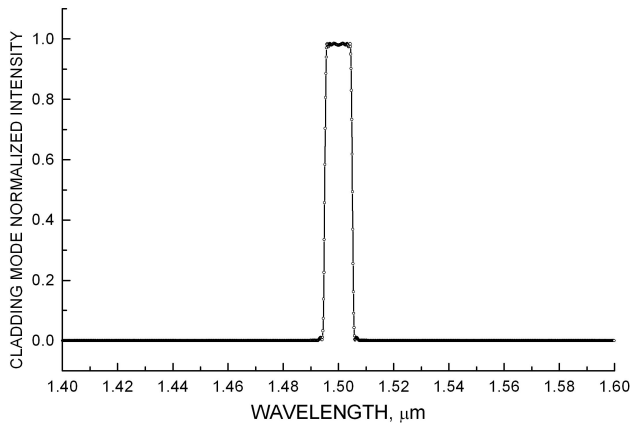


FIGURE 12. The synthesized spectrum of the cladding mode. The grating length  $L = 200$  cm.

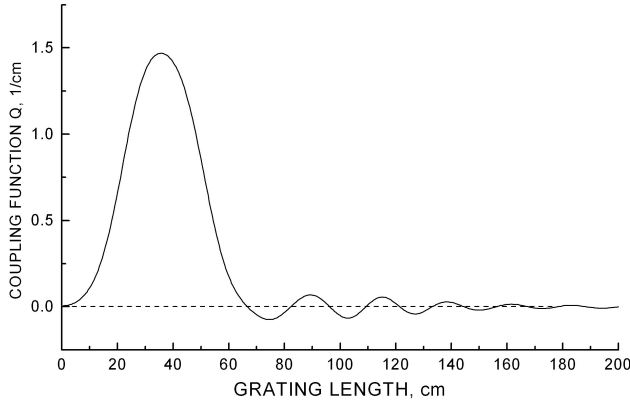


FIGURE 13. The synthesized coupling function  $Q(z)$  for the spectrum shown in Fig. 12.

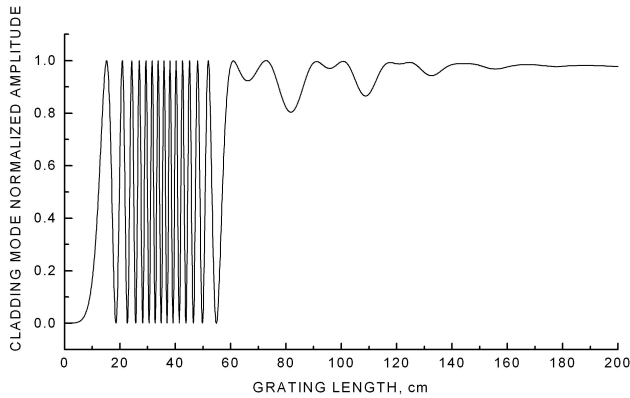


FIGURE 14. The spatial evolution of the cladding mode  $(|v(z)|^2 / |u_0|^2)$  in non-uniform LPG with the coupling function  $Q(z)$  shown in Fig.(4b), at  $\delta = 0.01 \text{ cm}^{-1}$ .

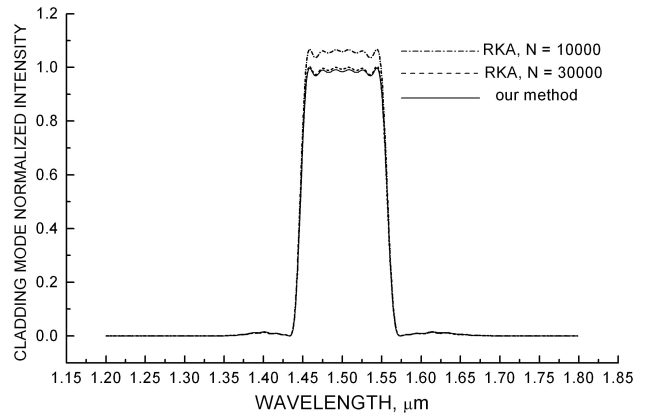


FIGURE 15. The synthesized spectrum of the cladding mode in non-uniform LPG with the slowly varying coupling function shown in Fig. 16, and at truncated length  $L = 15$  cm (this can be said only for the specific considered spectrum). The continuous curve was obtained by our GA; the dashed and short dot curves was obtained by RKA, at a different number of the discretization points ( $N$ ).

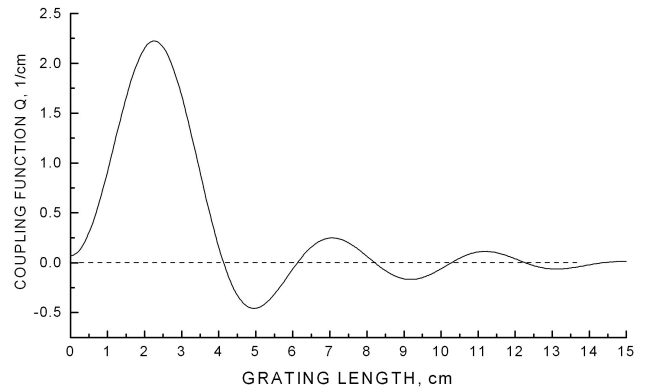


FIGURE 16. The synthesized coupling function  $Q(z)$  for the spectrum shown in Fig. 15. This case presents “realizable” non-uniform LPG for an ultra-wide-band filter.

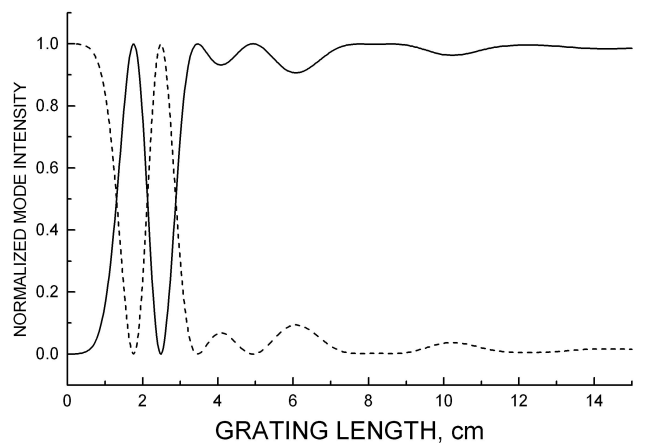


FIGURE 17. The spatial evolution of the cladding mode  $(|v(z)|^2 / |u_0|^2)$  in non-uniform LPG with the “realizable” coupling function  $Q(z)$  shown in Fig. 16 and 10b, at  $\delta = 0.01 \text{ cm}^{-1}$ .

The above problem associated with the ultra-wide band-pass filters can only be overcome if we use more soft requirements to the filter response. The realizable coupling function and its spectral response for ultra-wide filter with  $\Delta\lambda = 100$  nm are shown in Fig. 16 and 15, respectively. The results were obtained by limiting the number of *sinc* terms in Eq. (15), here  $M = 4$ , and by truncating the grating length. At these conditions the GA cannot synthesize “ideal”  $Q(z)$ ; however the structure, as can be seen from Fig. 17, possesses now more real characteristics, and the spectral response is quite acceptable.

To verify and estimate the efficiency of our method, we substituted the obtained coupling functions into a standard fourth-order Runge-Kutta algorithm (RKA) applied to Eq. (2). These results are shown in Fig. 9 and 15. One can see from the data that RKA, in general, reproduces the form of the spectra well, however, it can easily violate the law of conservation of energy because of the amplification effect described above. Moreover, it requires an extremely large number of the discretization points to eliminate this effect and to approach the maximum values of normalized curves to unity:  $N = 60000$  for an “ideal” filter (as one can see in Fig. 9 this number is still not sufficient) and  $N = 30000$  for an “realizable” filter. As the result, the computing time of the GA with incorporated RKA increases up to 380 minutes, compared to our two-step integration procedure that takes only 10-15 minutes with P-IV class PC. It should be noted, in the case that we want to synthesize a wide-band non-ideal filter

with a moderate peaked transmission, for example of 80% , the synthesis by the GA will take 1-2 minutes.

## 7. Conclusions

In this work, an efficient method for the synthesis of ultra-wide pass-band optical filters based on Long-Period Optical Fiber Gratings is described. The method is developed in the framework of a standard genetic algorithm where we incorporate the original, accurate, and very effective two-step procedure for the direct solution of the differential (Riccati) problem that covers the case of rapidly oscillating fields. The peculiarity of the method is that it is capable of providing quite accurate solutions at very hard conditions for the parameters of the structure. For example, the method works well even when the coupling function possesses a continuous profile with very rapid variations in space, compared to the grating period, as required for the filters with an ultra-wide and sharp-edged frequency response and 100% in-band transmission. The main advantage of our method compared to the IA, DLP, CLP methods proposed earlier, is that we use a quasi-analytical algorithm in the direct integration of the differential equations. Also, here we proposed to involve the relations of the conservation laws between the fields to improve the stability and accuracy of the synthesis procedure. As result, the method allows one to synthesize an “ideal” filter response in a reasonably (for GA) short time of 10-15 min.

---

\* Corresponding author: Oleg Kolokoltsev, e-mail: olegk@aleph.cinstrum.unam.mx Tel.: 56 22 86 02 Ext.1120, (UNAM), CCADET, Apartado Postal 70-186, 04510, CD Universitaria, México, D.F.

1. Proceedings of VII Europ. Conf. on Integrated Optics. *Netherlands*, Delft. Apr. 3-6, (1995).
2. F. Casagrande *et al.*, *Applied Optics* **41** (2002) 5238.
3. Turan Erdoran, *Journal of Light-wave Technology* **15** (1997) 1277.
4. H. Ke, K.S. Chiang, and J.H. Peng, *IEEE, Photonics Technology Letters*. **10** (1998) 1596.
5. Qing Lui, Kin Seng Chiang, and Vipul Rastogi, *IEEE, Journal of Light-wave Technology* **21** (2003) 3399.
6. Gia-Wei Chern and L.A. Wang, *J. Opt. Soc. Am. A* **19** (2002) 772.
7. J.R. Qian and H.F. Chen, *Electron Lett.* **34** (1998) 1132.
8. A.M. Vengsarka *et al.*, *Opt. Lett.* **21** (1996) 336.
9. C.K. Madsen and J.H. Zhao, *J. Wiley, New York* (1999).
10. K.A. Winick and J.E. Roman, *IEEE QE* **26** 11. (1990) 1918.
11. G.L. Lamb, *Elements of Soliton Theory* (New York: Wiley, 1980).
12. V.E. Zakharov and A.B. Shabat, *Sov. Phys. JETP*. **34** (1972) 62.
13. G.H. Song and S.Y. Shin, *J. Opt. Soc. Am.* **2** (1995) 1905.
14. C. Papachristos and P. Frangos, *J. Opt. Soc. Am. A* **19** (2002) 1005.
15. I. Kay, *Comm. Pure Appl. Math.* **13** (1960) 371.
16. P.V. Frangos and D.L. Jaggard, *IEEE, Trans. On Antennas and Propagation* **40** (1992) 399.
17. E. Peral, J. Capmany, and J. Marti, *IEEE J. of QE* **32** 12. (1996) 2078.
18. R. Feced, M.N. Zervas, and M.A. Muriel, *IEEE J. of QE* **35** 8 (1999) 1105.
19. R. Feced and M.N. Zervas, *J. Opt. Soc. Am. (A)* **17** (2000) 1573.
20. L. Poladian, *Opt. Lett.* **25** (2000) 787.
21. J. Skaar, L. Wang, and T. Erdogan, *IEEE J. of QE* **37** (2001) 165.
22. J. Skaar and Knut Magne Risvik, *J. of Lightwave Technology* **16** (1998) 1928.
23. G. Gormier and R. Boudreau, *J. Opt. Soc. Am. B* **18** (2001) 1771.
24. T. Bäck and H.P. Schefel, “Evolutionary Computation: An Overview”, in *Proc. IEEE International Conference on Evolutionary Computation* (1996) 20.

25. O.V. Kolokoltsev, C. Sánchez Pérez, and R. Amezcua Correa, *IEEE J. of Selected Topics in Quantum Electronics* **8** (2002) 1258.
26. A. Yariv, *IEEE J. of Quantum Electronics* **9** (1973) 919.
27. H. Kogelnik, "Theory of Optical Waveguides", in *Guided-Wave Optoelectronics*, T. Tamir (Ed. New York: Springer-Verlag, 1990).